Review of "Two different phytoplankton blooming mechanisms over the East China Sea during El-Niño decaying summers" by Lee et al.

Comment on egusphere-2024-3406 | Anonymous Referee #1:

This manuscript discusses an important issue of international interest. However, it is premature because of major flaws.

The major flaw is the erroneous assumption that riverine input is the primary source of nutrients(line 27). Much of the Introduction and Methods concerns river input. However, the Kuroshio Intermediate Water is the primary source of nutrients for the East China Sea shelf. Many papers substantiated this notion. The authors used the results presented in Figs. 2 and 3 to prove the importance of riverine inputs of nutrients. Yet, Figs. 2 and 3 only provided a good correlation between chlorophyll and nutrients that mostly did not come from rivers. Instead, the upwelling of nutrient-rich Kuroshio subsurface waters provided most of the nutrients. Of course, upwelling could be induced by the buoyance effect caused by the river water(e.g., Chen 2008, Acta Oceanologica Sinica, 27,133, 2008). To summarize, the so-called runoff-driven blooming mechanism is not caused by riverine nutrients. Instead, it is caused by buoyancy-driven upwelling and vertical mixing. BTW, validation is needed to substantiate the modeled results presented in these two figures.

Another factor worth mentioning is that the outflow of the South China Sea is the primary source of Kuroshio waters entering the East China Sea. During El Nino years, there is a more substantial outflow of the more nutrient-rich SCS water(e.g., Chen et al., Deep-Sea Res. I, 103,13, 2015), which may enhance productivity on the ECS shelf.

As a final note, many of the figures are not labeled correctly. Figures 1, 2, 3, 4, 5, 6, 9, and 10 are all related to anomalies, not the actual values. The "p" values should also be provided.

Response: We thank the reviewer for constructive and valuable comments and suggestions on our results. We have made substantial revisions to the manuscript in response to the referee's key comments.

We sincerely appreciate referee #1 for the comment that nutrient supply from the entrainment of subsurface waters via dynamic buoyancy upwelling induced by great out-flowing river plume is an important influence on phytoplankton blooms in the ECS region as well. Obviously, we missed this physical process in the original manuscript. By following the referee's suggestions, we have added a clarification to the manuscript to state that the runoff-driven mechanism also includes nutrient supply from the subsurface water entrainment due to buoyancy upwelling caused by enhanced river discharge during the El Niño decaying summers in the ECS continental shelves as follows:

(L139-145): In addition to direct riverine nutrient input, enhanced river discharge can deliver nutrients to the East China Sea (ECS) region through buoyancy-driven upwelling (Chen, 2008; Chen et al., 2003; Chen, 2000; Hill, 1998). When the outflowing river plume becomes more substantial than the incoming river discharge, subsurface waters are upwelled to maintain water balance. This process allows nutrient-rich Kuroshio subsurface waters to ascend along the ECS shelf edge, supplying essential nutrients to the region. Unlike wind-driven upwelling, this buoyancy-driven upwelling is governed by the physical properties of the subsurface waters in response to intensified river outflow.

(L170-174): Although the GFDL-CM2.1 ESM does not simulate P inputs from riverine inflows, it does account for P supply through the dynamic ascent of subsurface waters driven by buoyancy upwelling resulting from river discharge. Therefore, beyond analyses based on observational and reanalysis data, long-term model simulations enable us to comprehensively understand the phytoplankton blooming mechanisms in the ECS during the following summers of El Niño events.

Additionally, we have substantially revised the manuscript in response to the referee's comments. As the reviewer suggested, we discussed the role of nutrient transport through the Taiwan Strait (TS) (Huang et al., 2015; Zhang et al., 2015; Chen et al., 2015) by adding new analyses. In the revised manuscript, we have extensively addressed this by incorporating the nutrient transport mechanism through the TS (TS-transport-driven mechanism). Using nutrient data from Copernicus Marine Environment Monitoring Service (CMEMS) reanalysis and current data from Simple Ocean Data Assimilation (SODA) reanalysis, we calculated the meridional PO_4 transport during the summers of El Niño's decaying phase (refer to "Data and Method" for details).

As the referee noted, both observational and model results confirm that the composite analysis of meridional PO_4 transport through the TS shows significantly positive signals across the entire TS region during El Niño decaying summers (Figure R1). We have incorporated Figure R1a into Figure 1d in the main text to further illustrate the primary nutrient source in the ECS region. In addition, the model results demonstrate that the correlation between runoff (r = 0.59**; Figure R2a) and SCHL is weaker compared to the correlation between meridional PO_4 transport through the TS (represented as the blue diagonal box in Figure R1b) and SCHL (r = 0.68**; Figure R2b). In addition to the TS region index, zonally-averaged meridional PO_4 transport flux in TS and SCHL correlations at 26.5°N (120.5°E–122.5°E) and 27.5°N (121.5°E–123.5°E) also exhibit significantly high positive correlations of 0.66 and 0.57, respectively (Figure R3). Moreover, the distinction between the strong blooming and non-blooming groups reveals a pronounced difference in the magnitude of meridional PO_4 transport through the TS (Figure R4). We have incorporated Figure R2b and Figure R4 as Figure 6 in the main text. Therefore, we have added a paragraph to the

main text to describe the TS-transport-driven blooming mechanism based on the model results:

(L256-265): We also investigated the TS-transport-driven blooming mechanism, which is well known for its significant role in nutrient supply through the TS. We analyzed the meridional PO4 transport by comparing two groups as the same as Fig. 5, and found remarkably distinct differences between them (Figure 6a-c). Notably, within the TS, a strong positive (negative) signal was identified in the SB (NB) group. For the SB group, the nutrient flux exhibits a significant positive signal reaching the target region, potentially supplying large amount of nutrients and making a substantial contribution to SCHL blooming in the ECS region. Furthermore, a positive correlation of 0.68—higher than the runoff-driven mechanism—was identified between the anomalous SCHL blooming magnitude in the target region and the meridional PO4 transport index indicated by the blue diagonal box in the TS region (Figure. 6d). This underscores the critical role of the TS-transport-driven mechanism in fostering nutrient into the ECS region.

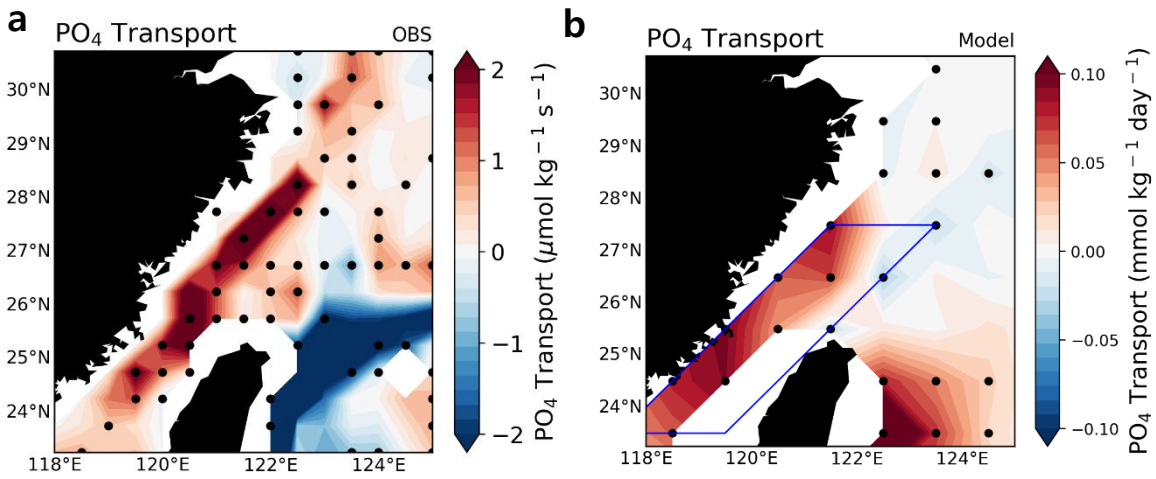

Figure R1. Composite map of meridional PO_4 transport anomalies during El Niño decaying summer season in the Taiwan Strait (TS) for all El Niño cases in observations (Left Panel) and model results (Right Panel). All the black dots where the responses are statistically significant at the 90% (in observations) and 95% (in model results) confidence level, determined using the bootstrap method.

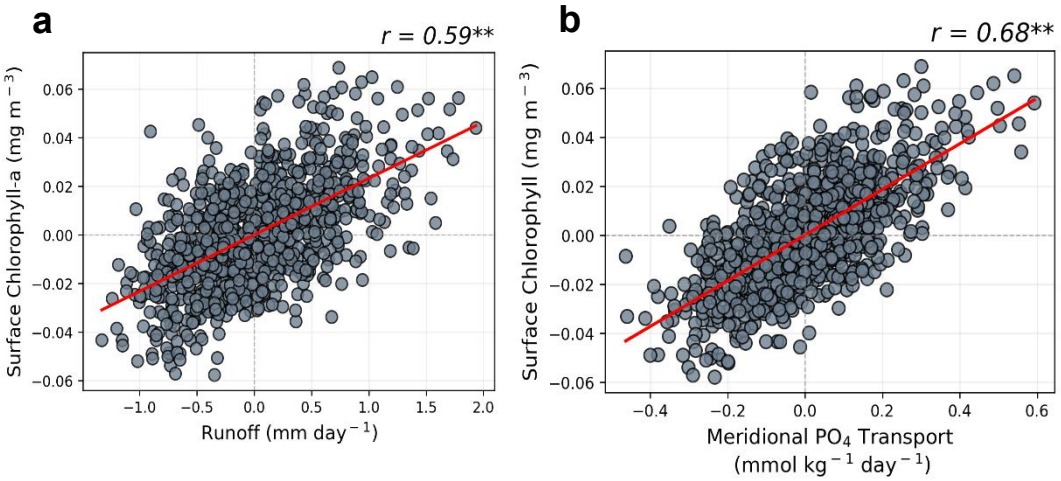

Figure R2. The relationship between area-averaged runoff and SCHL anomalies over the target region (Figure R2a), and the relationship between area-averaged meiridonal PO_4 transport and SCHL anomalies over the target region (Figure R2b).

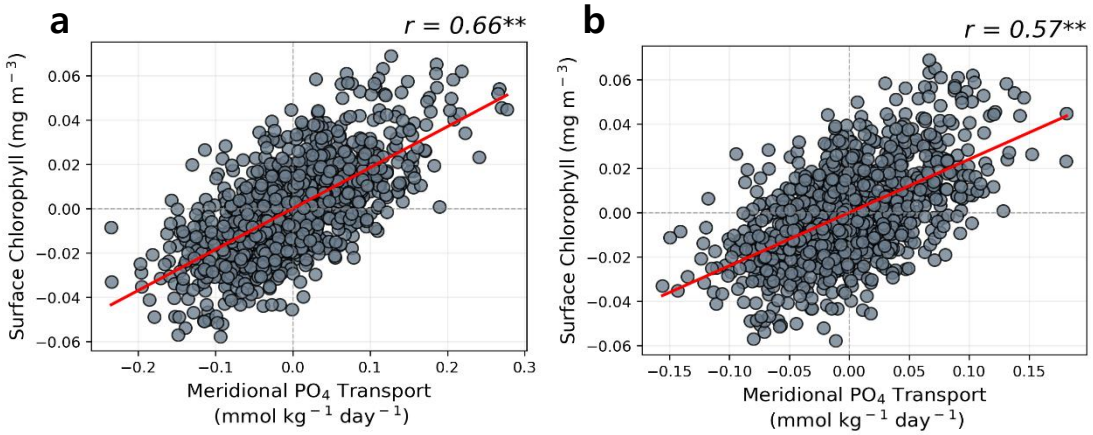

Figure R3. The relationship between zonally-averaged meridional PO4 transport (26.5˚N-120.5˚E-122.5˚E; Left Panel / 27.5˚N – 121.5˚E-123.5˚E; Right Panel) and SCHL anomalies over the target region.

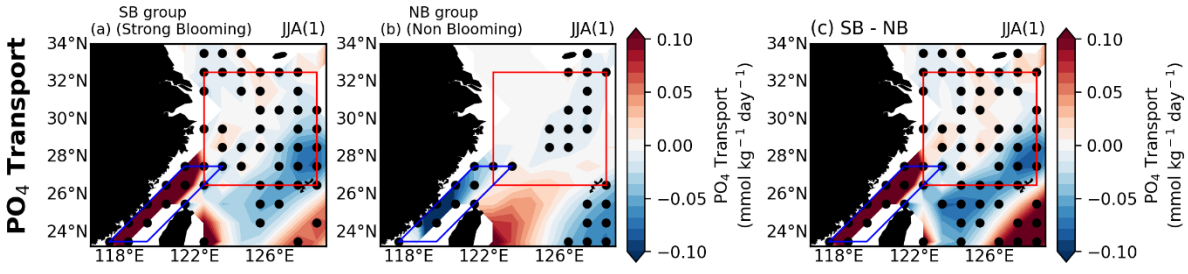

Figure R4. Composite maps of meridional PO_4 transport anomalies during El Niño decaying summer for Strong Blooming group (Figure R4a), Non-Blooming group (Figure R4b) and the difference between the two groups (Figure R4c).

The overall structure of the manuscript has been substantially reorganized. Instead of comparing the two previously proposed blooming mechanisms—"runoff-driven" and "upwelling-driven"—we have revised the manuscript to first re-evaluate the known mechanisms: ”runoff-driven” and “TS-transport-driven”. Subsequently, we incorporate both observational and modeling evidence to support the upwelling-driven mechanism, emphasizing the importance of understanding all these complex phytoplankton blooming mechanisms.

Additionally, in the revised manuscript, we assessed the relative contributions of three mechanisms using a regression method instead of the joint-composite analyses (Figure R5, Table R1; We added Figure R5 and Table R1 as Figure 9 and Table 1 in the manuscript respectively). We normalized all variables and conducted multiple regression for three mechanism indices at each grid point of SCHL anomalies across the target region. And, we quantified the relative contributions of three mechanisms by multiplying the linear regression coefficients between the Nino3.4 index and each mechanism index by their multiple regression coefficients respectively (Eq. 1; We added it as Eq. 4 in the manuscript).

The results indicate that both the Runoff- and the TS-transport-driven mechanism have the most significant contributions to the intensity of SCHL blooming in the target region. Although the Ekman Upwelling-driven mechanism exhibits a lower contribution compared to the others, it still exerts a meaningful influence on about half of the other mechanisms. Spatially, the Runoff-driven mechanism primarily affects the central area of the target region (Figure R5a), while the TS-transport-driven mechanism plays a major role along a southwest-northeast diagonally (Figure R5b). In contrast, the Ekman Upwelling-driven mechanism uniformly influences the overall target region (Figure R5c). Especially, the runoff- and the TS-transport-driven mechanism contribute similarly to the SCHL blooming intensity in the target region.

Although the Ekman upwelling-driven mechanism accounts for approximately 40 to 47% of the others, it still exerts a significant influence (Table R1). Consequently, we have replaced the paragraph that calculated the relative contribution for each mechanism from the joint-composite analyses previously we used to the regression method as follows:

(L313-349): So far, we have conducted a comprehensive evaluation and analysis of the complex mechanisms driving phytoplankton blooms in the ECS during the summers following the decaying phase of El Niño events. In addition to the runoff- and TS-transport-driven mechanisms suggested in previous studies, we introduced the Ekman upwelling-driven blooming mechanism. Subsequently, we quantified the relative contributions of these three mechanisms based on regression methods using (Eq. 4) as follows:

$$\frac{dChl}{dNino3.4}(\alpha) = \frac{\partial Chl}{\partial Runoff} \times \frac{dRunoff}{dNino3.4} + \frac{\partial Chl}{\partial TS-transport} \times \frac{dTS-transport}{dNino3.4} + \frac{\partial Chl}{\partial Ekman-Upwelling} \times \frac{dEkman-Upwelling}{dNino3.4} + residual \quad (4)$$

Firstly, we normalized all variables and conducted the multiple regression with respect to SCHL index in the target region as the dependent variable and three mechanism indices as independent variables. Secondly, we calculated each term by multiplying the linear regreesion coefficient between Nino3.4 index and each mechanism index by the corresponding multiple regression coefficient for each mechanism index. The combined effects of the three mechanisms and the residual term collectively account for the variation of the SCHL index in the ECS region with respect to the El Niño events. Therefore, each term indicates how changes in three mechanism induced by ENSO cycle (as indicated by the Nino3.4 index) affect on phytoplankton blooms in the ECS region. The results show the effect of runoff-driven mechanism and the TS-transport mechanisms to SCHL blooming intensity in the target region are comparable (Table 1). In the case of the Ekman upwelling mechanism, it accounts for about 40% to 47% of contributions comapred to the other two mechanisms, yet still exerts a meaningful influence as well.

Table R1. Relative contributions of three mechanisms to SCHL blooming in the target region.

	α	Runoff	TS-transport	Ekman Upwelling
Contribution	0.511	0.152	0.138	0.065

Additionally, we identified their spatial contributions to further elucidate the effects of each mechanism within the target region (Figure 9). We conducted multiple regression for three mechanism indices at each grid point of SCHL anomalies across the target region. Following the same way examined above, we calculated the spatial contributions by multiplying the linear regression coefficents of each mechanism with repsect to the Nino3.4 index. The results showed that the runoff-driven mechanism exhibited the strongest contribution at the center of the target region, driven by direct riverine nutrient inflow (though the model doesn't simulate P input) and nutrient supply through buoyancy upwelling induced by river discharge (Figure 9a). In contrast, the TS-transport-driven mechanism significantly contributes along a southwest-northeast diagonal direction, aligning with nutrient transport via the TS from the SCS (Figure 9b). Additionally, the newly proposed Ekman upwelling-driven mechanism, while relatively lower in overall contribution, shows significant and uniformly distributed impacts across the target region (Figure 9c). These results suggest that all mechanisms can affect comprehensively to induce phytoplankton blooms in the ECS during the following summers of the decaying phase of El Niño events. Therefore, considering all mechanisms is essential for accurately predicting the intensity of phytoplankton blooms.

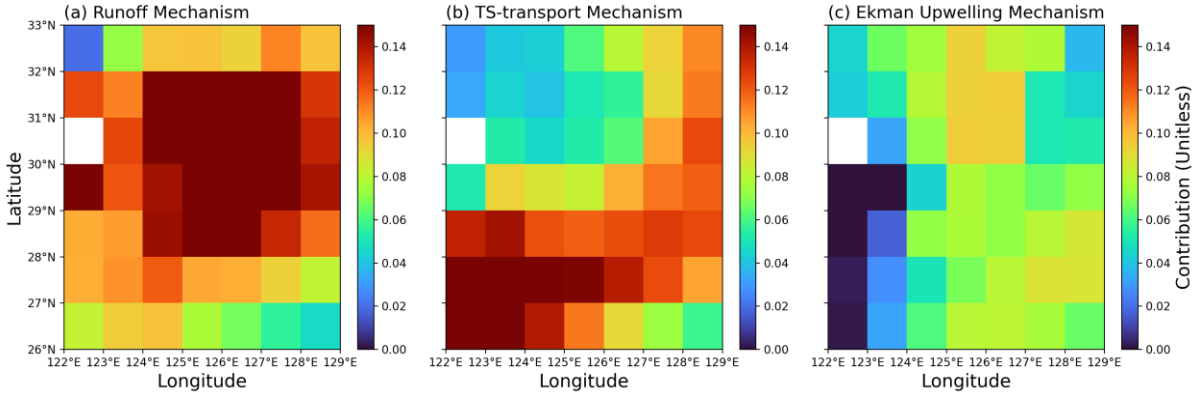

Figure R5. Relative contributions of three mechanisms to SCHL blooming in the target region during summers following the decaying phase of El Niño events **(a)** Runoff-driven mechanism **(b)** TS-transport-driven mechanism **(c)** Ekman upwelling-driven mechanism.

We have revised the title of the manuscript to **"Phytoplankton Blooming Mechanisms over the East China Sea during El Niño Decaying Summers"** to better reflect the scope and findings of our study.

Additionally, we have annotated all correlation analyses to emphasize statistical significance: a star (*) was added next to r values with a p-value below 0.05, and double stars (**) was added for r values with a p-value below 0.01.

We believe that these substantial revisions comprehensively address the referee's concerns and enhance the scientific value of the manuscript.

Reference

Chen, C. A.: Buoyancy leads to high productivity of the Changjiang diluted water: a note, Acta Oceanol. Sin., 27, 133–140, 2008.

Chen, C. T. A.: The Three Gorges Dam: Reducing the upwelling and thus productivity in the East China Sea, Geophys. Res. Lett., 27, 381–383, https://doi.org/10.1029/1999GL002373, 2000.

Chen, C. T. A., Liu, C. T., Chuang, W. S., Yang, Y. J., Shiah, F. K., Tang, T. Y., and Chung, S. W.: Enhanced buoyancy and hence upwelling of subsurface Kuroshio waters after a typhoon in the southern East China Sea, J. Mar. Syst., 42, 65–79, https://doi.org/10.1016/S0924-7963(03)00065-4, 2003.

Chen, C. T. A., Yeh, Y. T., Chen, Y. C., and Huang, T. H.: Seasonal and ENSO-related interannual variability of subsurface fronts separating West Philippine Sea waters from South China Sea waters near the Luzon Strait, Deep. Res. Part I Oceanogr. Res. Pap., 103, 13–23, https://doi.org/10.1016/j.dsr.2015.05.002, 2015.

Hill, A. E.: Buoyancy effects in coastal and shelf seas, Sea, 21–62, 1998.

Huang, T. H., Chen, C. T. A., Zhang, W. Z., and Zhuang, X. F.: Varying intensity of Kuroshio intrusion into Southeast Taiwan Strait during ENSO events, Cont. Shelf Res., 103, 79–87, https://doi.org/10.1016/j.csr.2015.04.021, 2015.

Zhang, W., Zhuang, X., Chen, C. A., and Huang, T.: The impact of Kuroshio water on the source water of the southeastern Taiwan Strait: numerical results, Acta Oceanol. Sin., 34, 23–34, https://doi.org/10.1007/s13131-015-0720-x, 2015.